

is greater than for protons. We do not understand the origin of these effects, but if they are verified by further experiments, their implications are rather important. In particular, $\sigma_R(E)$ needs to be measured and understood theoretically for heavier projectiles.

We would like to thank J. Blair, H. Britt, J. Cramer, and R. Nix for valuable conversations. This work was funded by the U. S. Department of Energy.

¹See, for example, W. Hess, *Rev. Mod. Phys.* **30**, 365 (1958).

²J. F. Dicello and G. Igo, *Phys. Rev. C* **2**, 488 (1970); R. F. Carlson *et al.*, *Phys. Rev. C* **12**, 1167 (1975); W. F. McGill *et al.*, *Phys. Rev. C* **10**, 2237 (1974); J. J. H. Menet *et al.*, *Phys. Rev. C* **4**, 1114 (1971); R. Goloskie and K. Straugh, *Nucl. Phys.* **29**, 474 (1962); P. Kirkby and W. T. Link, *Can. J. Phys.* **44**, 1847 (1966).

³P. U. Renberg *et al.*, *Nucl. Phys.* **A183**, 81 (1972).

⁴H. A. Bethe, *Phys. Rev.* **57**, 1125 (1940).

⁵C. W. deJager *et al.*, *At. Data Nucl. Data Tables* **14**, 479 (1974).

⁶W. T. H. van Oers, *Phys. Rev. C* **10**, 307 (1974).

⁷S. Mayo *et al.*, *Nucl. Phys.* **62**, 393 (1965).

⁸The experimental value of 346 mb for $d + {}^{12}\text{C}$ at 279 MeV/nucleon [L. M. C. Dutton *et al.*, *Phys. Lett.* **16**,

331 (1965)] can be compared with the elastic-scattering optical-model value of 397 mb for the same system at 180 MeV/nucleon [T. Sawada, *Nucl. Phys.* **74**, 289 (1965)].

⁹A. Chaumeaux *et al.*, *Nucl. Phys.* **A267**, 413 (1976); G. Alkhozov *et al.*, *Nucl. Phys.* **A280**, 365 (1977); R. Beurtey *et al.*, Commissariat à l'Énergie Atomique Report No. CEA N2026 (unpublished).

¹⁰ $\alpha + {}^{40}\text{Ca}$ at 1.37 GeV is from W. R. Coker *et al.*, *Phys. Lett.* **64B**, 403 (1976): $(V, W, R_v, R_w, R_c, A_v, A_w) = (-9.53, -69.1, 1.15, 1.17, 1.35, 0.70, 0.69)$. $d + {}^{16}\text{O}$ at 698 MeV is from J. R. Shepard (private communication), and in Centre d'Études Nucléaires de Saclay, *Compte Rendu d'Activité*, 1976-1977, Report No. CEA-N-2026 (unpublished), p. 113: $(V, W, R_v, R_w, R_c, A_v, A_w) = (21.23, -15.45, 1.133, 1.217, 1.20, 0.409, 0.428)$. $\alpha + {}^{12}\text{C}$ at 1.37 GeV is obtained by using the search program GENOA (F. Perey, unpublished): $(V, W, R_v, R_w, R_c, A_v, A_w) = (-9.53, -45.16, 0.804, 1.295, 1.38, 0.70, 0.45)$.

¹¹D. A. Goldberg *et al.*, *Phys. Rev. C* **10**, 1362 (1974); G. Hauser *et al.*, *Nucl. Phys.* **A182**, 1 (1972); G. Hauser *et al.*, *Nucl. Phys.* **A128**, 81 (1969); B. Tatischeff and I. Brissaud, *Nucl. Phys.* **A155**, 89 (1970); P. Gailard *et al.*, *Nucl. Phys.* **A131**, 353 (1969); S. M. Smith *et al.*, *Nucl. Phys.* **A207**, 273 (1973); F. Hinterberger *et al.*, *Nucl. Phys.* **A111**, 265 (1968); L. Bimbot *et al.*, *Nucl. Phys.* **A210**, 397 (1973); M. D. Cooper *et al.*, *Nucl. Phys.* **A218**, 249 (1974); H. J. Apell *et al.*, *Nucl. Phys.* **A246**, 477 (1975).

Nuclear Spins of the Isomers ${}^{191m-185m}\text{Hg}$ Determined by On-Line Quantum-Beat Spectroscopy

H. Kremmling, P. Dabkiewicz, H. Fischer, H.-J. Kluge, T. Köhl, and H. A. Schuessler^(a)
Institut für Physik, Universität Mainz, Mainz, Federal Republic of Germany

(Received 25 June 1979)

The nuclear spins of the very neutron-deficient ${}^{191m-185m}\text{Hg}$ isomers were measured on line at the mass separator ISOLIDE at CERN using pulsed-laser excitation and observation of the time-resolved quantum beats from selected hyperfine-structure states. The spins of these isomers are with $I = \frac{13}{2}$ equal to those of the long-lived isomers ${}^{199m-193m}\text{Hg}$ already known. The persistence of this spin value for eight isomers is explained by the model of rotation-aligned coupling.

This Letter reports the application of quantum-beat spectroscopy to the determination of the nuclear spins of the neutron-deficient isomers ${}^{191m,189m,187m,185m}\text{Hg}$. The experiment was performed with mass-separated mercury isomers produced at the ISOLDE II isotope separator which is on line with the CERN 600-MeV proton synchrocyclotron.¹ In previous work² the hyperfine structure (hfs) and the isomer shift in the $6s^2 1S_0 - 6s6p 3P_1$, $\lambda = 2537\text{-Å}$ line were studied by Doppler-limited fluorescence spectroscopy. A

huge isomer shift was found at $A = 185$ which is due to the coexistence of slightly deformed oblate and strongly deformed prolate nuclear shapes. In the present experiment, quantum beats were observed from hfs Zeeman levels of single hfs states which allowed the determination of the nuclear spins. This independent measurement ideally complements the previous laser fluorescence results, which could only determine the first three of the four hfs structure parameters, namely, the magnetic dipole coupling constant A ,

the electric quadrupole coupling constant B , and the center of gravity of the hfs multiplet W_j , but not the nuclear spin I . In addition, the observed beat frequencies readily identify a particular hfs level in a complex spectrum where lines from different isomers and isotopes may overlap.

Quantum beats are observed by tuning the laser to resonance with the hfs level of interest and then monitoring the time evolution of the superposition of coherent atomic states produced by a short broad-band laser pulse. Such beats have been studied in the spontaneous decay of a variety of excited states,³ however, only a few experiments yielded new spectroscopic data. In this Letter we report the first application of the quantum-beat method to the spectroscopy of short-lived isotopes far from β stability. The precision is limited only by the natural lifetime of the excited atomic state and makes the Doppler-free observation of the hfs of radioactive elements possible.

The isotopes of interest are excited by a short resonant-laser pulse in a weak external magnetic field. In such a case a coherent superposition of excited hfs Zeeman levels belonging to a single hfs level is produced. The time evolution of this atomic coherence leads to the quantum beats superimposed on the fluorescent decay at the various Bohr frequencies determined by the energy difference of the excited hfs Zeeman states according to $\nu = (E_{\mu'} - E_{\mu})/h$. Without integration over time, Breit's theory⁴ of resonance fluorescence describes the pulse excitation and yields in the limit of short pulses for the instantaneous rate S of photons emitted:

$$S \propto \sum_{\mu\mu'mm'} f_{\mu m} f_{m\mu'} g_{\mu'm'} g_{m'\mu} \times \exp[-i(E_{\mu'} - E_{\mu})t/h - (\Gamma_{\mu'} + \Gamma_{\mu})t/2], \quad (1)$$

where the f 's and g 's are the excitation and fluorescence matrix elements for electric dipole radiation between the ground states m and excited states μ , and Γ is the decay constant $\Gamma = 1/\tau$ with τ being the natural lifetime of the excited state. For the transition studied, the lifetime of the excited $6s6p\ ^3P_1$ state is⁵ $\tau = 115(2)$ nsec and much longer than the laser pulse, so that the application of the simple Eq. (1) is justified.

When the laser light is polarized perpendicular to the external magnetic field H , the simultaneous σ^+ and σ^- excitation leads to $\Delta m = 2$ beats. Their frequency ν is then given by $\nu = 2\gamma'H$, where the gyromagnetic ratio γ' is defined by $\gamma' = g_F\mu_B/h$ and g_F is approximately given by $g_F = g_J \{ [F(F+1) - J(J+1) - I(I+1)] / 2F(F+1) \}$. Equation (1) takes then the simple form

$$S(t) \propto \exp(-t/\tau) [1 - B \cos(2\pi\nu t)], \quad (2)$$

where B is the modulation amplitude determined by the dipole matrix elements.

The isomers studied are produced by spallation in a molten lead target.¹ The 70-keV ions from the mass separator ISOLDE II are collected on a molybdenum foil for about two half-lives, then evaporated as thermal atoms into a quartz cell and excited by a pulsed frequency-doubled dye laser system (Fig. 1). The ultraviolet output is 2.5 kW in a 3-nsec long pulse with a spectral width of about 1 GHz. The experiment is carried out in two steps. First, the location of the various hfs levels for a particular mass number is found by scanning the laser over the absorption line of the unstable isotope. The laser frequency is calibrated by observing simultaneously the Zeeman-shifted resonance light from a sample of stable even isotopes in a reference cell (Fig. 2). In the second step, the laser is set on resonance with the hfs level of interest and the beat signal is observed. Most measurements were carried out on the $F = I$ hfs state of the various isomers, where the maximum signal is expected. In cases of low atom densities in the resonance cell, photon counting is employed and the counts are buf-

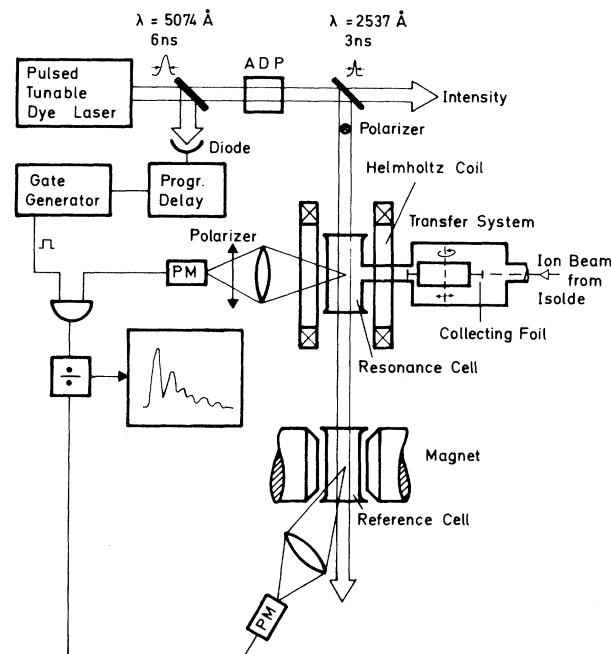


FIG. 1. Schematic diagram of the on-line laser-spectroscopy experiment.

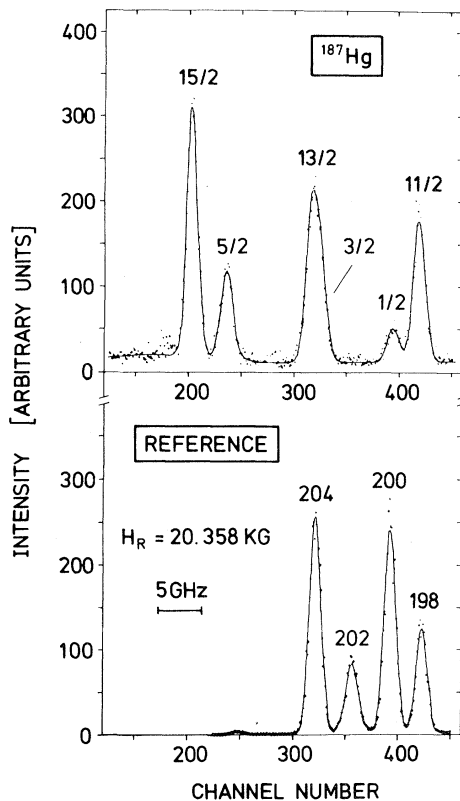


FIG. 2. Fluorescent light from the excited hfs levels of the nuclear ground and the isomeric states in the $\lambda = 2537 \text{ \AA}$ line of ^{187}Hg (upper part) of the σ^+ Zeeman components of the even stable mercury isotopes in a magnetic field of $H_R = 20.358 \text{ kG}$ (lower part) vs laser frequency.

fered in a fast data register. In the case of more abundant isotopes the current of the photomultiplier is fed into a 10-bit analog-to-digital converter (ADC) which is gated by a gate generator programmed with a variable time delay. The fast data register or the ADC is read by a computer using CAMAC instrumentation. The data are normalized to constant light intensity with the photomultiplier signal of the reference cell.

With a laser repetition rate of 50 Hz, reasonable statistics are obtained within a time ranging from a few minutes up to about 30 min. However, in the case of short-lived isotopes the obtainable vapor densities are low, e.g., for ^{185}Hg ($T_{1/2} = 27 \text{ sec}$) the density is only about 10^7 atoms/cm^3 . As a consequence, the fluorescent light is small compared to the direct laser light pulse scattered off the walls of the resonance cell and hence the photomultiplier running at high gain is disturbed by this pulse. In order to reduce the

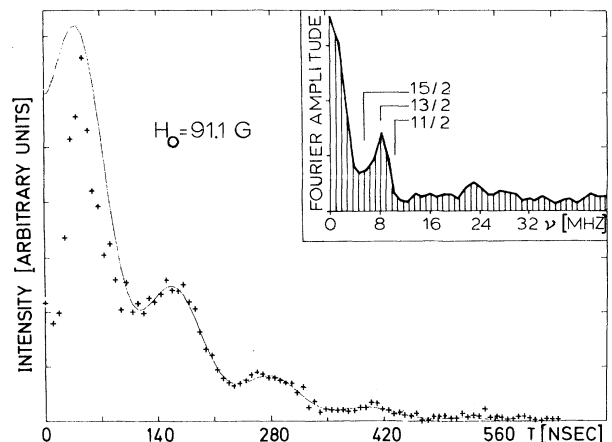


FIG. 3. Quantum-beat signal from the $F = I = \frac{13}{2}$ hfs level of ^{187m}Hg . The inset shows the corresponding Fourier transform of the beat pattern. For comparison the frequencies expected of a $F = I$ hfs level of the spin values $I = \frac{11}{2}$ and $I = \frac{15}{2}$ are indicated.

overloading and subsequent afterpulsing, the photomultiplier is turned off during the laser pulse by a 100-V blanking pulse applied to the focusing electrode. Still, the beat pattern is heavily disturbed during the first 80 nsec after laser excitation. Figure 3 shows as an example a measurement of the $F = I$ hfs state of ^{187m}Hg where the solid line represents a fit by Eq. (2) omitting the first twelve data points. The fit yields a beat frequency of $\nu = 8.3(3) \text{ MHz}$ leading to a gyromagnetic ratio of $\gamma' = 45.8(1.0) \text{ kHz/G}$. Although this value does not, even within the error bars, exactly coincide with the theoretical value of $\gamma'(F = I - \frac{13}{2}) = 43 \text{ kHz/G}$, this value unambiguously determines the isomeric spin to be $I = \frac{13}{2}$. For comparison, the gyromagnetic ratios for the neighboring spin quantum numbers $I = \frac{11}{2}$ and $I = \frac{15}{2}$ are $\gamma' = 58 \text{ kHz/G}$ and $\gamma' = 33 \text{ kHz/G}$. The above deviation is explained by a modulation of the anode current due to the direct laser pulse and the blanking pulse. A test without radioactive atoms yields a frequency of this modulation of $21(3) \text{ MHz}$. The relative signal height $B_{\text{exp}} = 0.38$ is only 77% of the theoretical value of $B_{\text{theor}} = 0.49$ and is due to the finite solid angle detected by the photomultiplier, the smoothing of the beat pattern by the gate width of 20 nsec, and a small π -polarization component in the σ^+ excitation pulse.

A fast-Fourier analysis with the Cooley-Tuckey algorithm was also performed to obtain an indication of the presence of other frequency components. The result for ^{187m}Hg is shown in the inset

of Fig. 3 and displays besides the contribution at $\nu=0$ MHz mainly one additional frequency at about $\nu=8$ MHz. This corresponds to $\gamma'=43.5$ kHz/G and again yields for a measurement in a $F=I$ hfs term a nuclear spin of $I=\frac{13}{2}$. The small peak around $\nu=23$ MHz agrees with the contribution from the blanking pulse on the detection electronics.

Very similar quantum beats were observed for the other isomers $^{191m-185m}\text{Hg}$ leading to $I=\frac{13}{2}$ in all cases. The results of the present experiment are listed in Table I. The same spin values were found earlier for the long-lived isomers $^{199m-193m}\text{Hg}$ so that an $I=\frac{13}{2}$ state was observed for eight isotopes over a chain of 14 mass numbers. The single-particle model offers a simple explanation for the persistence of this spin value: In the mass region of interest the relevant neutron orbits $3p_{3/2}$, $2f_{5/2}$, $3p_{1/2}$, and $1i_{13/2}$ are within a few 100 keV of each other. In general, the pairing energies are larger than these energy differences and determine the actual neutron configuration. It is, therefore, expected that neutron pairs fill the high-spin states first, while unpaired neutrons are expected in the low-angular-momentum levels. This reasoning is supported by the measured values of the spins of the nuclear ground states for the mercury isotopes between $187 \leq A \leq 205$ ($I=\frac{1}{2}$, $\frac{3}{2}$, and $I=\frac{5}{2}$). Hence it can be concluded that, (1) the isomers differ essentially by an $i_{13/2}$ neutron pair and (2) in this mass region the successive filling of the $i_{13/2}$ shell with these pairs is observed. However, the measured spectroscopic quadrupole moments of the isomers ($0.5 \text{ b} \leq Q_s \leq 1.5 \text{ b}$)² as well as the $B(E2)$ values of the neighboring even isotopes ($0.11 \leq |\beta| \leq 0.15$)⁶⁻⁹ point to collective effects. Using the Nilsson model, a contradictory prediction for the nuclear spin is obtained. For the heavy isomers the $[606, \frac{13}{2}]$ level reaches the Fermi surface for $\beta > 0$. Reorientation measurements in this mass region show, however, an oblate deformation.^{6,7} According to the Nils-

son diagram, the $[606, \frac{13}{2}]$ level is below the Fermi surface, while the same level with a ($\Omega = \frac{1}{2}$) projection of the nuclear angular momentum on the symmetry axis of the nucleus $[660, \frac{1}{2}]$ reaches the Fermi surface. For strong coupling of the unpaired neutron to the oblate core $I=\Omega$ is expected which contradicts the measured $I=\frac{13}{2}$. However, the $I=\frac{13}{2}$ isomers are neither spherical nor strongly deformed but represent typical transition nuclei. In the case of a nucleon with large angular momentum j the Coriolis force may overcome the coupling of the valence particle to the core and j aligns itself parallel to the rotation axis R of the nucleus. In the rotation-aligned coupling scheme¹⁰ the projection α on the angular momentum with respect to R becomes sharp and $\alpha=j=\frac{13}{2}$ is expected irrespectively of the filling of the $i_{13/2}$ subshell. This interpretation of the persistence of the isomeric spin $I=\frac{13}{2}$ is supported by the observation of decoupled bands,¹¹ the sign of the spectroscopic quadrupole moment,² and the trend of the odd-even staggering parameter.¹²

Finally, a comparison of the quantum-beat method used in this experiment with other methods is made. The main advantages of the quantum-beat method are the short time needed for a measurement which is in the order of the lifetime of the excited state and the simplicity of the apparatus. In comparison, a double-resonance experiment needs rather strong rf magnetic fields to saturate the signal in a high-spin excited hfs level. The Hanle effect requires a careful analysis of the effects which influence the linewidth, such as collisions in the excited state, coherence narrowing, distortion by the scattered laser pulse, imperfect compensation of Earth's magnetic field, and not optimally adjusted geometry. Only the phase, B and τ of Eq. (2), changes in a quantum-beat experiment in these cases but the beat frequency is not influenced.

The authors thank E.-W. Otten for his involvement in this work, H. H. Stroke for fruitful discussions, and the ISOLDE Collaboration for continuous help and advice. This work was supported by the Deutsches Bundesministerium für Forschung und Technologie, the Deutsche Forschungsgemeinschaft, and the U. S. National Science Foundation. This work has been submitted as part of a thesis by one of us (H. Kremmling).

TABLE I. Experimental data for the neutron-deficient Hg isomers.

A	$T_{1/2}$	I
191m	50.8 min	13/2
189m	8.7 min	13/2
187m	1.6 min	13/2
185m	27 s	13/2

(^a) On leave from the Department of Physics, Texas A & M University, College Station, Texas 77843.

¹H. L. Ravn, L. C. Carraz, J. Denimal, E. Kugler, M. Skarestad, S. Sundell, and L. Westgaard, Nucl. Instrum. Methods **139**, 276 (1976).

²P. Dabkiewicz, F. Buchinger, H. Fischer, H.-J. Kluge, H. Kremmling, T. Kuehl, A. C. Mueller, and H. A. Schuessler, Phys. Lett. **82B**, 199 (1979).

³For a review on quantum beats see S. Haroche, *Topics in Applied Physics* (Springer, Berlin, Hamburg, and New York, 1976), Vol. 13.

⁴G. Breit, Rev. Mod. Phys. **5**, 91 (1933).

⁵A. Lurio, Phys. Rev. **140**, A1505 (1965).

⁶R. Kalish, R. R. Borchers, and H. W. Kugel, Nucl.

Phys. **A147**, 161 (1971).

⁷A. Bockisch, K. Bharuth-Ram, A. M. Kleinfield, and K. P. Lieb, Z. Phys. A **289**, 231 (1979).

⁸D. Proetel, R. M. Diamond, and F. S. Stephens, Phys. Lett. **48B**, 102 (1974).

⁹N. Rud *et al.*, Phys. Rev. Lett. **31**, 1421 (1973).

¹⁰F. S. Stephens, Rev. Mod. Phys. **47**, 43 (1975).

¹¹D. Proetel, D. Benson, A. Gizon, J. Gizon, M. R. Maier, R. M. Diamond, and F. S. Stephens, Nucl. Phys. **A226**, 237 (1974).

¹²H. H. Stroke, D. Proetel, and H.-J. Kluge, Phys. Lett. **82B**, 204 (1979).

Rate Theory for the Four-Photon Ionization of Cs near the 6F Resonance

Burke Ritchie

Department of Chemistry, University of Alabama, University, Alabama 35486

(Received 11 May 1979)

A previously presented narrow-bandwidth theory is used to interpret recent data on the four-photon ionization of Cs near the 6F resonance. The theory is based on treating the amplitude of the radiation field as a constant relative to its rapid phase oscillations. The ionization rate adiabatically follows a pulsed amplitude leading to maximum ionization for times at which the pulse develops sufficient intensity to shift the 6S → 6F transition into resonance.

In a previous paper¹ (I) a formalism was presented based on treating the amplitude of the classical radiation field $b(t)$, which is slowly varying in the time, as a constant relative to the oscillatory part of the field, which is rapidly varying in the time. Using this adiabatic approximation, the Fourier integral of the field $A(t)$ is proportional to a δ function in frequency space,

$$a(\omega) = (2\pi)^{-1} \int_{-\infty}^{\infty} dt e^{i\omega t} A(t) \simeq b(t) \delta(\omega - \omega_p), \quad (1)$$

where ω_p is the constant photon frequency and only the absorptive component of the field is considered. Thus the field depends on $b(t)$ *parametrically*. This form illustrates the single-mode character expected for a very-narrow-bandwidth field such as that of the recent experiment by Morellec and co-workers² (II), where the bandwidth is about $2 \times 10^{-3} \text{ cm}^{-1}$.

In the experiment of II the flux F depends on the time. This time dependence is described by multiplying F by a dimensionless Gaussian shape function $G(t)$, with a 37 ns width at half maximum, which generates a maximum F corresponding to an intensity of 10^9 W cm^{-2} at the center of the pulse t_0 . It is the purpose of the present paper to evaluate the slowly varying field amplitude $b(t)$,

proportional to $[G(t)F]^{1/2}$, as adiabatically following the rapidly varying oscillatory part whose use in the dynamical problem has led to a rate. That is, we replace $b(t)$ in Eq. (1) by $[2\pi G(t)F/\alpha\omega_p]^{1/2}e$. This quantity occurs as a parameter in the time-independent rate. The success of the present adiabatic-following approximation in describing the time dependence of the ionization yield data of II will be demonstrated below and illustrates how a time-independent rate theory^{1,3-6} can be used to describe temporal phenomena in laser-induced ionization.

The flux also depends on the focal volume (Figs. 3 and 11 of II). This dependence is given by multiplying the maximum flux (corresponding to an intensity of 10^9 W cm^{-2}) developed at t_0 by a dimensionless shape function $F_s(x, y, z)$, where this function is normalized to 1 at the center of the focal volume, or $F_s(0, 0, 0) = 1$ (Appendix of II). In this paper we multiply $G(t)F$ above by $F_s(0, 0, z)$, where $G(t)$ and $F_s(0, 0, z)$ are constructed from the information given in II [Figs. 11(a), 11(b), and 14]. Our rate^{1,3-6} $R_4(z, t)$ for the four-photon ionization of Cs near the 6F resonance, for a given time t in the development of the pulse along a path z through the center of the focal volume,